



**Politecnico
di Torino**

Master's Degree Thesis in Environmental and Land Engineering

Graduation session:

October 2024

On the Turbulence Properties of Channel Flows

Supervisors:

Prof. Costantino Manes

Candidate:

AMIR YOUSEFABADI

CONTENTS:

1	INTRODUCTION.....	5
2	LITERATURE.....	7
3	METHODOLOGY.....	9
	3.1 Overall facility description	9
	3.2 Description of the test section.....	13
	3.3 Description of LDA.....	15
	3.4 Calculation Bulk velocity and Reynold number.....	20
	3.5 Welch method and Power Spectral Density (PSD).....	22
4	RESULTS.....	25
	4.1 Point A (5 mm from the bottom or center)	25
	4.2 Point B (2.5 mm from the bottom)	29
	4.3 Comparison of point A and point B.....	32
5	CONCLUSION.....	34
6	ACKNOWLEDGMENTS.....	35
7	REFERENCES.....	36

Figures:

Figure 1. The whole <i>hydraulic</i> system.....	9
Figure 2. Tank for water storage.....	10
Figure 3. Smaller pump.....	11
Figure 4. Bigger pump.....	11
Figure 5. Convergence and Air release.....	12
Figure 6. Control valve	13
Figure 7: Test section	14
Figure 8: BSA flow software	16
Figure 9: The whole system of LDA	17
Figure 10: When LDA is on.....	18
Figure 11: LDA beams intersection (visually alignment)	19
Figure 12: Velocity Guage.....	20
Figure 13: Velocity vs Time for $Re=135$, point A (5mm from the bottom)	25
Figure 14: Velocity vs Time for $Re=1800$, point A (5mm from the bottom)	25
Figure 15: PSD vs f at logarithmic scale for point A, $RE=1400$	27
Figure 16: PSD vs f , at non logarithmic scale for point A, $RE=1400$	28
Figure 17: turbulent intensity vs RE , for point A, before and after removing noises.....	29
Figure 18: Velocity vs Time for $Re=135$, point B (2.5mm from the bottom)	30
Figure 19: Velocity vs Time for $Re=1800$, point B (2.5mm from the bottom)	30
Figure 20: turbulent intensity vs RE , for point B, before and after removing noises.....	32
Figure 21: turbulent intensity vs RE comparison, for points A and B, after removing noises.....	33

Tables:

Table 1: Pont A, bulk and mean velocity, SD (before and after removing noises)26

Table 2: Pont A, bulk and mean velocity, SD (before and after removing noises)31

LIST OF ABBRERATIONS AND SYMBOLS:

Re [-]	Reynold number
U[m/s]	Bulk velocity
D[m]	Hydraulic diameter
ν [m ² /s]	Kinematic viscosity
T.I[-]	Turbulent intensity
S. D	Standard Deviation

1: INTRODUCTION:

The definitions of laminar, transitional, and turbulent flow are fundamental concepts in fluid dynamics, each characterized by distinct flow patterns and behaviors. Understanding these types of flow is crucial for various engineering applications, as they significantly influence drag, energy consumption, and mixing properties. Laminar flow is smooth and orderly, with fluid particles moving in parallel layers. Transitional flow occurs between laminar and turbulent states, marked by instabilities in the flow. The transition is influenced by factors such as flow acceleration and disturbances, leading to a mix of laminar and turbulent characteristics. Turbulent flow is chaotic and irregular, with eddies and vortices. It typically occurs at high Reynolds numbers. This flow regime significantly increases drag and energy consumption, making it critical to understand for efficient system design (1).

My research has focused on the fluid regime (laminar, transitional, or turbulent) and the turbulent intensity within these regimes. The Reynolds number, a dimensionless quantity, defines the fluid regime. It measures the ratio of inertial forces to viscous forces within a fluid experiencing relative internal movement due to varying fluid velocities.

While other parameters (dynamic viscosity, fluid density) involved in calculating the Reynolds number remained constant throughout my experiments, the velocity was the variable parameter. The experiments were conducted in a closed, rectangular duct with a smooth surface, using water as the fluid. Laser Doppler Anemometry (LDA) was employed to measure velocity. By determining the velocity, Reynolds number, and streamwise turbulent intensity, I was able to predict the stream behavior.

Identifying the type of regime is very important in water treatment using membranes. This experiment serves as a basis for another experiment conducted in the same test section with membranes to determine the suction rate of the filtered water.

The turbulent regime plays a crucial role in enhancing suction rates during filtration processes at membranes. This is primarily due to its impact on mass transfer and boundary layer dynamics, which are essential for efficient filtration. Turbulent flow conditions significantly increase the

mass transfer coefficient, which is vital for effective filtration. higher suction velocities lead to improved mass transfer rates (2).

2: LITERATURE:

In fluid dynamics, the term transition refers to the process by which a fluid flow changes from a laminar state to a turbulent state. Laminar flow is characterized by smooth, orderly fluid motion in parallel layers, with minimal mixing between them. In contrast, turbulent flow is chaotic and characterized by irregular fluctuations and mixing.

The transition from laminar to turbulent flow is a complex process influenced by various factors, including the Reynolds number, which is a dimensionless quantity representing the ratio of inertial forces to viscous forces within the fluid. ($Re = \frac{\text{inertial forces}}{\text{viscous forces}} = \frac{\bar{u} * D}{\nu}$)

\bar{u} =average velocity, D=hydraulic diameter, ν =kinematic viscosity.

The transition process typically involves several stages. Initially, small disturbances in the laminar flow grow due to instabilities. These disturbances can be triggered by factors such as surface roughness, flow velocity, and pressure gradients. As these disturbances amplify, they lead to the formation of turbulent spots, which eventually merge and spread, resulting in fully developed turbulence. Understanding this transition is crucial for predicting and controlling fluid behavior in various engineering applications, such as pipeline transport, water treatment.

Turbulence is inherently chaotic, making it challenging to describe and predict. However, statistical methods provide a framework for analyzing turbulent flows. One of the fundamental concepts in the statistical description of turbulence is averaging. By averaging the fluctuating quantities over time or space, we can extract meaningful information about the flow's overall behavior. The mean velocity is a key statistical measure used to describe turbulent flows. It represents the average velocity of the fluid at a given point over a specified period.

$$\text{Mean velocity} = \bar{u} = \frac{1}{T} \int_0^T u(t) dt$$

where $u(t)$ is the instantaneous velocity at time (t), and (T) is the period.

In addition to the mean velocity, other statistical measures such as the root mean square (RMS) of velocity fluctuations (standard deviation (SD)), turbulence intensity, and Reynolds stresses are

used to characterize turbulence. These measures provide insights into the energy distribution, mixing efficiency, and momentum transfer within the turbulent flow.

In recent decades, numerous experiments have focused on turbulent channel flows. Open channel flows, commonly observed in nature, are a frequent subject of study.

While most experiments have concentrated on open channel flows or circular pipes, many industrial applications involve non-circular shaped channels. To address this gap, a study focused on the relationship between mean velocity and turbulent intensity in ducts, comparing results to the log law. However, existing experiments have primarily explored turbulent progression in fully developed streams at high Reynolds numbers. (3)

A critical aspect of fluid behavior is understanding the transition to turbulent flow. Determining the Reynolds number at which this transition occurs is essential for various applications. For instance, in wastewater treatment, filtration efficiency, which is crucial for public health, is directly related to the turbulent intensity and degree of turbulent development of the fluid. The suction rate (the amount of water filtered) is also influenced by longitudinal velocity. This underscores the importance of accurately identifying the flow regime.

The experiment described in this experiment aims to investigate the relationship between turbulent intensity and Reynolds number in a closed duct section. The goal is to determine the specific Reynolds number at which the flow transitions from laminar to turbulent.

3: METHODOLOGY:

3.1: Overall Facility Description:

The entire experiment was conducted at the hydraulic laboratory of Polytechnic University of Turin. The hydraulic plant, pictured in Figure 3.1, is primarily constructed from stainless steel 316L for enhanced durability. This material offers superior resistance to corrosion.



Figure 1: The whole hydraulic system

The system consists of a 1 m³ tank filled with municipal water (figure.2).



Figure 2: Tank for water storage

A chiller maintains a constant water temperature throughout the tests. Feed water is drawn from the tank by two parallel multistage pumps, offering a combined maximum flow rate of 2.4 l/s. These pumps operate independently, each mounted on a separate pipe branch equipped with isolation ball valves. To achieve lower flow rates suitable for laminar and transitional regimes, the smaller pump is used. Conversely, the larger pump is employed for turbulent flow conditions (Figure.3,4)



Figure 3: Smaller pump



Figure 4: Bigger pump

Immediately downstream, the two pipelines converge into a single main pipeline. A flow meter positioned on the horizontal section of the main pipeline measures the water velocity. The pipeline then continues until reaching a diffuser. As the pipeline ascends from the ground, its diameter increases.

This convergence (figure.5) can generate air bubbles within the flow, which are removed by an air release valve.



Figure 5: Convergence and Air release

Following this, there is a chamber, followed by another fluid dynamic diffuser before the test section. This configuration allows for undisturbed development of boundary layers within the test section. Downstream of the test section, a pipe with a smaller diameter is used to enhance flow rate control within the test section.

Flow rate and velocity adjustments for achieving the desired Reynolds number are accomplished through two methods. The first method involves adjusting the pump frequency - a higher frequency naturally leads to a higher flow rate. The second method utilizes a control valve installed downstream of the test section (Figure.6). By employing these methods, we can precisely adjust the flow rate and obtain the desired bulk velocity.

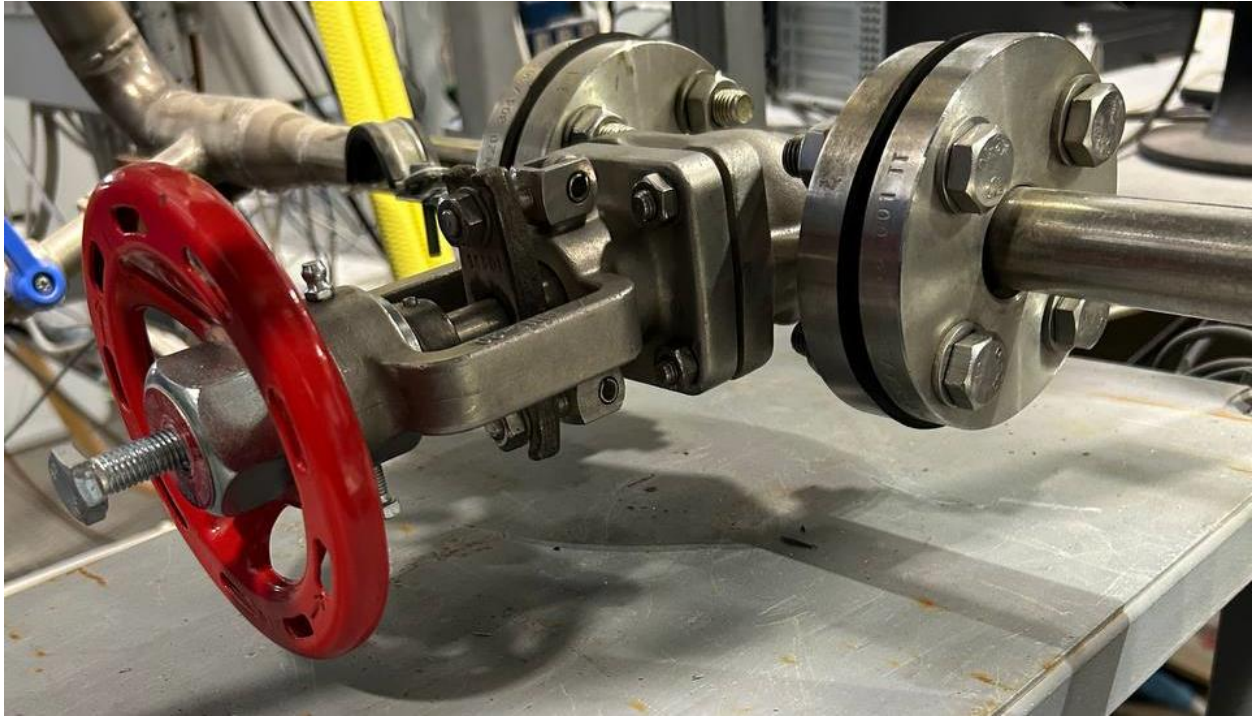


Figure 6: Control valve

3.2: Description of the Test Section:

The most critical component of the system is the test section. It consists of a rectangular channel, measuring 1.45 meters in length, 0.2 meters in width, and 0.01 meters in height. The channel is constructed entirely of transparent plexiglass, enabling optical access for Laser Doppler Anemometry (LDA). This configuration allows for precise velocity measurements at various locations within the channel. Figure (7) provides a more detailed view of the test section.



Figure.7: Test section

Within the test section, we aim to create a stream where fluid characteristics, such as velocity and turbulent intensity, are independent of the longitudinal (streamwise) coordinate. To achieve this, a crucial concept is the aspect ratio (width-to-height ratio) of the channel. Extensive research has been conducted to determine the optimal aspect ratio for ensuring stream independence.

For example, a study on open channel flow concluded that both the aspect ratio and the dimensionless curvature radius significantly influence turbulent kinetic energy. (4)

This finding is essential for understanding energy dissipation in turbulent flows, which has applications in river management and habitat conservation.

Another study employed Direct Numerical Simulations (DNS) to analyze flow past a circular cylinder confined within a rectangular duct at a Reynolds number of $Re = 630$. The investigation included ducts with widths of 4.44, 10, and 20 times the cylinder diameter, along with an infinite channel. The researchers observed that only ducts with widths exceeding 20-cylinder diameters achieved a flow structure similar to that of an infinite channel, with minimal variation in asymmetric structures along the span. (5)

Based on these findings, we can conclude that an aspect ratio (width-to-height) of 20 or greater guarantees independence of velocity and turbulent intensity from the longitudinal coordinate within the test section. In this experiment, the channel width is 20 cm, while the height is 1 cm, resulting in an aspect ratio of 20. This ensures self-similarity in longitudinal coordinates, allowing us to install the Laser Doppler Anemometer (LDA) at any point within the channel for accurate velocity measurements.

3.3: DESCRIPTION OF LDA:

The signal analysis was carried out with a Dante Dynamic Burst Spectrum Analyzers (BSA F600-2D) and a BSA flow software v.6.5 was used. (Figure.8)

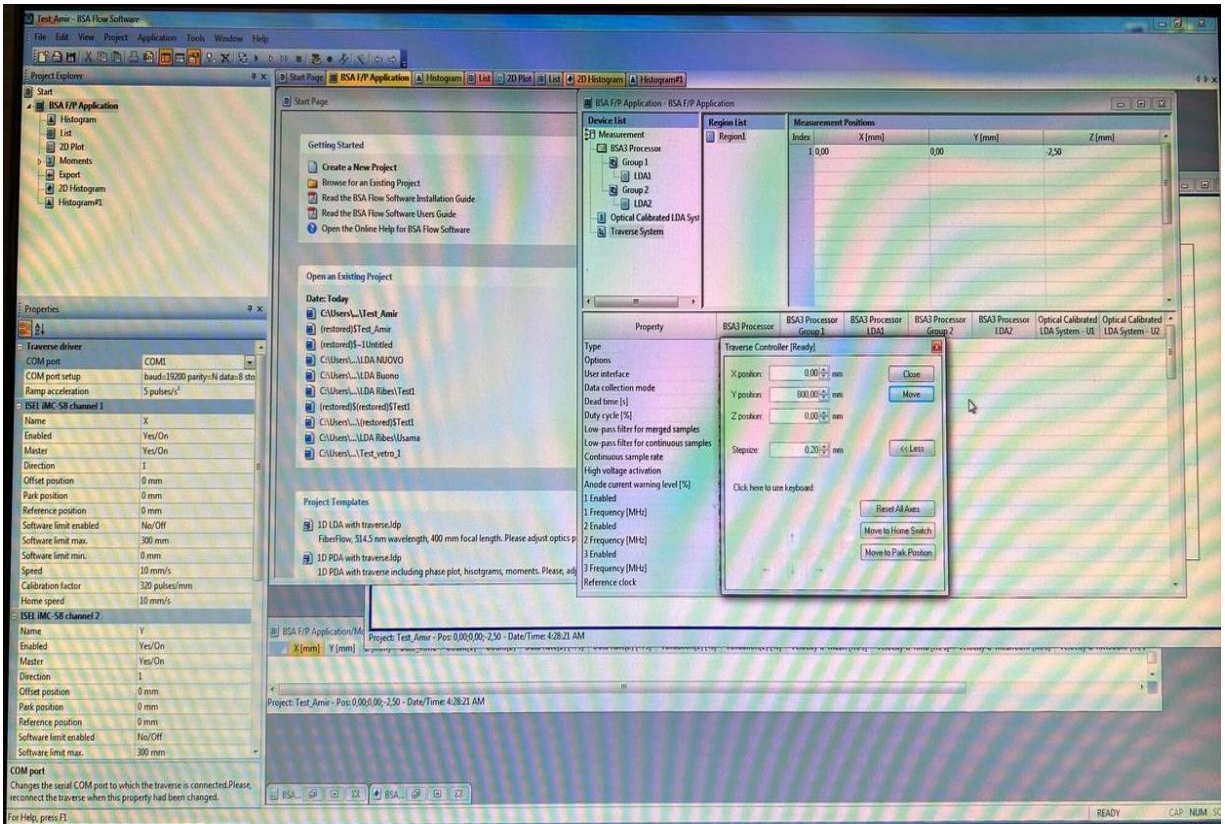


Figure 8: BSA flow software

For coordinates in the test section, there are three axes: the x-axis, which is in the direction of the streamwise flow of water (longitudinal); the y-axis, which is in the direction of the width of the test section; and the z-axis, which is in the direction of the height of the test section.

Before commencing measurements, it is essential to verify the vertical alignment of the test section. Velocity measurements were taken at two specific points, point A and point B which their coordinates are described at below. For both points, the measurement location was precisely at the center of the test section with regard to width of test section, corresponding to $y = 10$ cm.

The first point (point A) had coordinates of $x = 83.5$ cm, $y = 10$ cm, and $z = 5$ cm from the bottom of the test section and for the second point (point B) has the same coordinates for x and y but with

$z=5\text{mm}$. When the LDA is activated (figure.9,10) to measure velocity at the desired point, the two laser beams intersect at a specific point. This intersection point must correspond exactly to the coordinates of the target point. To ensure accurate alignment, we visually observed the intersection point from a top perspective, as illustrated in the figure below. (Figure.11)



Figure 9: The whole system of LDA

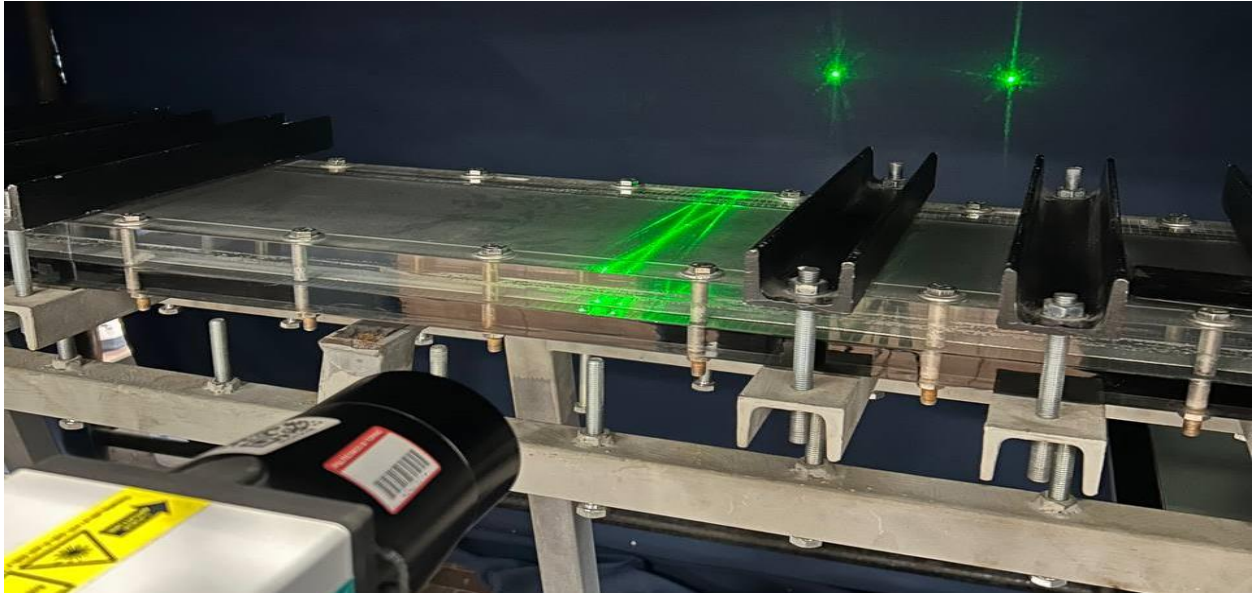


Figure 10: When LDA is on

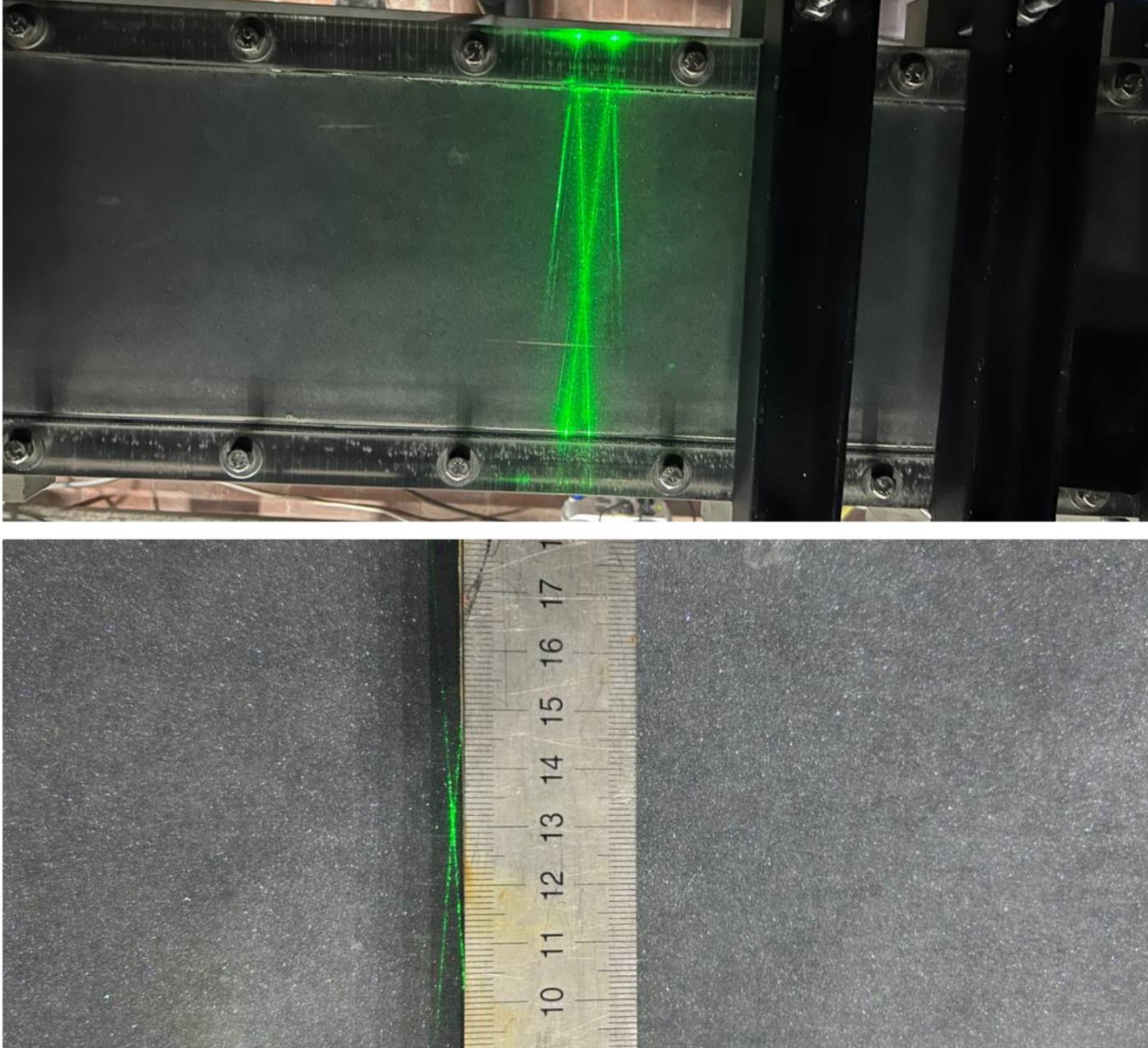


Figure 11: LDA beams intersection (visually alignment with ruler)

Once the LDA is confirmed to be measuring the intended point, the experiment proper begins. The primary objective is to measure velocities and subsequently calculate the corresponding Reynolds number.

To determine the Reynolds number, we need the bulk velocity, which can be directly read from a velocity gauge installed upstream of the test section (Figure.12). By adjusting the pump frequency and the control valve position (Figure 6), we can achieve a broad range of bulk velocities. However, there are limitations to this approach.

The pump frequency must be higher than 20 Hz to provide sufficient power for pumping water to the elevated test section. Additionally, adjusting the control valve opening affects the pressure within the test section. This pressure is limited to a maximum of 0.8 bar to prevent cracks in the test section. We consider these factors when adjusting the bulk velocity.



Figure 12: Velocity Guage (flow meter)

3.4: Calculating Bulk Velocity and Reynolds Number:

To calculate the bulk velocity, we utilize the Reynolds number. The Reynolds number is calculated using the formula:

$$Re = U * D / \nu$$

where:

- Re is the Reynolds number
- U is the bulk velocity
- D is the hydraulic diameter (in this case, the half-height of the test section, which is 5 mm)
- ν is the kinematic viscosity of water

While the Reynolds number does not directly involve temperature, temperature affects kinematic viscosity (ν). To ensure that all parameters involved in defining the Reynolds number remain constant except for velocity, we must maintain a consistent temperature and kinematic viscosity throughout the experiments.

A chiller attached to the reservoir (tank) maintains a constant temperature. This is crucial because the frictional forces and other factors involved in pumping water can cause a gradual increase in temperature over time. The chiller effectively addresses this issue. The temperature during all experiments was maintained between 19°C and 20°C and kinematic viscosity is considered equal to 1.0016×10^{-6} .

So now is the time to do tests for both points. We activate the pump and adjust it alongside the control valve to achieve the desired velocities based on the velocity gauge readings. This allows us to cover a range of Reynolds numbers, from the lowest (135) to the highest (1800).

Once the target velocity corresponding to a specific Reynolds number is reached, we activate the LDA to measure the velocity at the desired point. Each test is conducted for a duration of 5 to 7 minutes. After the measurement period ends, we collect the velocity time series data.

From the time series data, we calculate the mean velocity for each test, which corresponds to a specific Reynolds number. Using both the time series data and the mean velocity, we then calculate the standard deviation for each test (Standard deviation is a measure of the amount of variation or dispersion in a set of values. It quantifies the average distance of each data point from the mean of the dataset). To calculate the standard deviation in a velocity time series, first, the mean velocity must be calculated. Then, we sum up the squares of the differences between each measured velocity and the mean velocity. Finally, we take the square root of this sum. In this way, the standard deviation is calculated.

When the standard deviation is calculated for each Reynolds number, all of them are divided by the maximum mean velocity among all the mean velocities for all Reynolds numbers. For two points, from Reynolds 135 to 1800, the mean velocities are calculated, and the maximum mean velocity belongs to point A (5mm) for the highest Reynolds number (1800), which is equal to 0.48837. Therefore, all the standard deviations are divided by this number. This way, we have the standard deviation for all Reynolds numbers at two points.

For each point (A and B), we plot a graph of turbulent intensity versus the corresponding Reynolds number. These graphs allow us to identify the ranges of Reynolds numbers that define the laminar, transitional, and turbulent regimes for each measurement location.

3.5: PWELCH METHOD AND POWER SPECTRAL DENSITY(PSD):

LDA works by directing two laser beams that intersect at a small measurement volume within the flowing water. When particles in the flow pass through this region, they scatter light. The scattered light undergoes a frequency shift due to the motion of the particles (the Doppler effect). This shift is proportional to the velocity of the particles. The light scattered by these particles is detected and converted into an electronic signal. The frequency of this signal is directly related to the velocity of the fluid flow.

In a velocity-time series, the signal corresponds to the velocity information of the particles. The LDA continuously measures and records the velocity of particles passing through the measurement volume, creating a time series of velocity data.

There is a concept named PSD, which is a measure of the power (or variance) of a signal as a function of frequency. It shows how the energy of the velocity fluctuations is distributed across different frequencies. Essentially, it tells you how much of the velocity signal's variance, divided by the corresponding frequency, is contained at a particular frequency.

Mathematically, the PSD of a signal ($u(t)$) is defined as the Fourier transform of its autocorrelation function($R(\tau)$).

$$S(f) = \frac{1}{\pi} \int_0^{\infty} e^{-i2\pi f\tau} R(\tau) d\tau$$

- $S(f)$, represents the power spectral density(PSD) as a function of frequency (f).
- $R(\tau)$, is the autocorrelation function of the signal ($u(t)$), which measures the similarity between the signal and a delayed version of itself as a function of the delay(τ).
- $e^{-i2\pi f\tau}$, is the complex exponential function used in the Fourier transform.
- The integral is taken over all possible time lags .

Each value of $S(f)$ in the PSD is scaled so that:

Variance(y)= $\int_0^{\infty} S(f)d(f)$, which it means the area under the curve PSD vs f gives the variance which is equal to $\overline{u'^2}$.

Using the Welch method, we can draw the graph of PSD versus frequency, and the area under this curve gives us the variance of the signal, which is the energy characteristic of the signal. The Welch method is used for calculating PSD.

The code in MATLAB used for Welch has five parameters that need to be defined, as shown below:

`[psd, f] = pwelch(velocity, window, overlap, nFFT, fs);`

- velocity: The velocity time series data.
- window: The number of elements that the velocity time series data is divided into.
- overlap: The number of overlapping elements between subsequent windows.
- nFFT: The number of points in the FFT, typically the same as the window length.
- fs: The sampling frequency of the signal.

Since velocity measurements are obtained using LDA, some level of noise is inevitable. To remove this noise and improve the accuracy of our turbulent intensity data, we employ the Welch method. After applying this method, we obtain new graphs of normalized turbulent intensity versus

Reynolds number for both points. These graphs can then be combined into a single plot to visually determine which point exhibits higher turbulent intensities.

4: RESULTS:

4.1: Point A (5mm from the bottom or center):

The following two figures illustrate the velocity time series for the lowest and highest Reynolds numbers at point A as two examples. (figure.13,14)

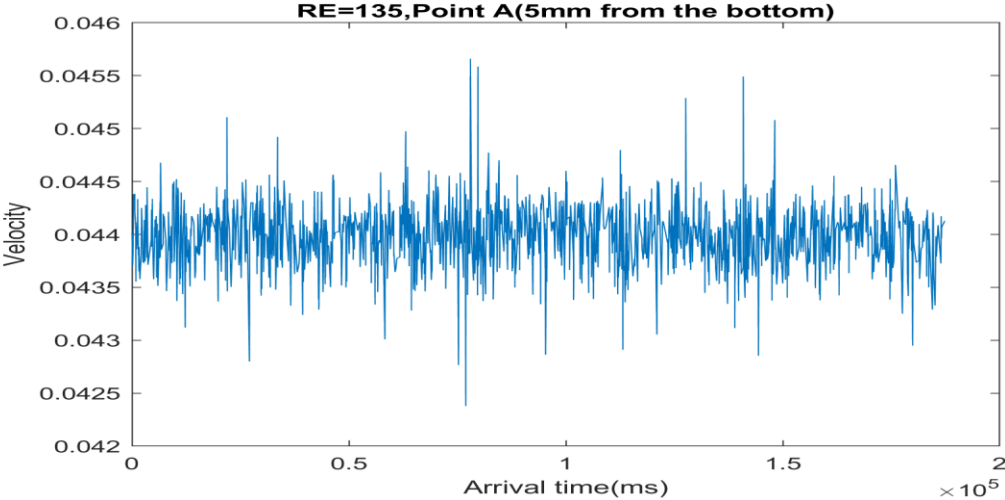


Figure 13: Velocity vs Arrival time for Re=135, point A (5mm from the bottom)

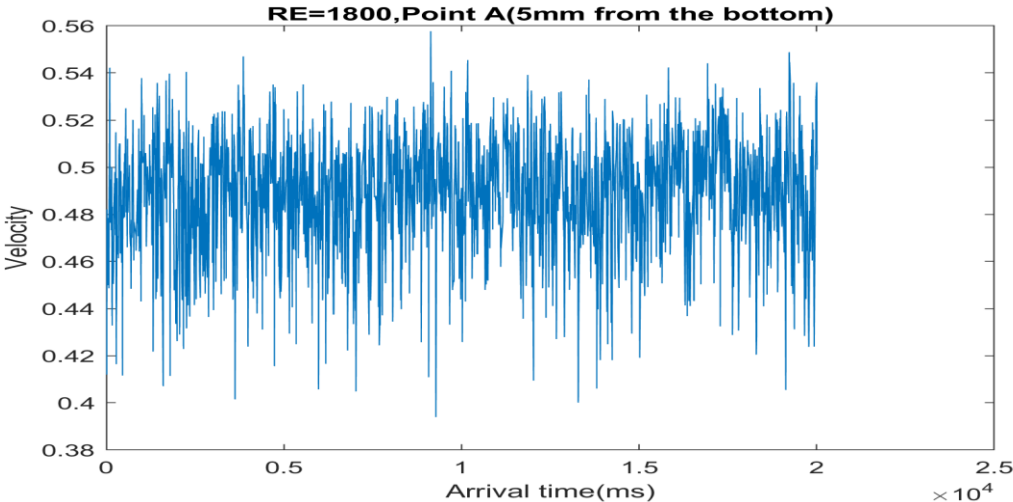


Figure 14: Velocity vs Arrival time for Re=1800, point A

By comparing these two velocity time series, we can observe that as velocity increases, there is a corresponding increase in fluctuations.

The table below presents the Reynolds numbers, bulk velocities, mean velocities, and standard deviations (SD) before and after removing white noises for each test at point A(5 mm from the bottom).(Table.1)

Test	RE	Bulk Velocity(m/s)	Mean velocity(m/s)	SD(before removing white noises)	SD (after removing white noises)
1	135	0.027	0.043959	0.00074878	0.00065
2	150	0.03	0.049586	0.0017223	0.000252
3	200	0.04	0.064866	0.00042933	0.000276
4	250	0.05	0.083337	0.0037296	0.0003057
5	300	0.06	0.10001	0.0043958	0.000451
6	350	0.070	0.11688	0.0012863	0.000651
7	400	0.080	0.13174	0.005885	0.000991
8	450	0.09	0.14734	0.0038239	0.0015
9	500	0.1	0.1679	0.009905	0.0014
10	550	0.11	0.17969	0.0021657	0.002
11	600	0.12	0.20212	0.0079384	0.0029
12	650	0.13	0.22262	0.0041901	0.0041
13	700	0.14	0.23825	0.021215	0.0043
14	750	0.15	0.2581	0.024196	0.0053
15	800	0.16	0.27529	0.030306	0.0084
16	850	0.17	0.28651	0.03239	0.0111
17	900	0.18	0.28769	0.03475	0.0209
18	950	0.19	0.28961	0.037493	0.0215
19	1000	0.2	0.29609	0.034588	0.0246
20	1200	0.24	0.33579	0.030094	0.0242
21	1400	0.28	0.39011	0.029636	0.0223

22	1600	0.32	0.43917	0.037801	0.0248
23	1800	0.36	0.48837	0.032683	0.0186

Table.1: Point A, Re, Bulk velocity, Mean velocity, Standard Deviation (before and after removing noises)

For obtaining the SD after removing white noise, as explained in the methodology section, we first draw the PSD vs. frequency in a logarithmic scale to visually identify from which frequency onwards there is white noise. As an example, for Reynolds 1400 at point A, this is shown in Graph 15.

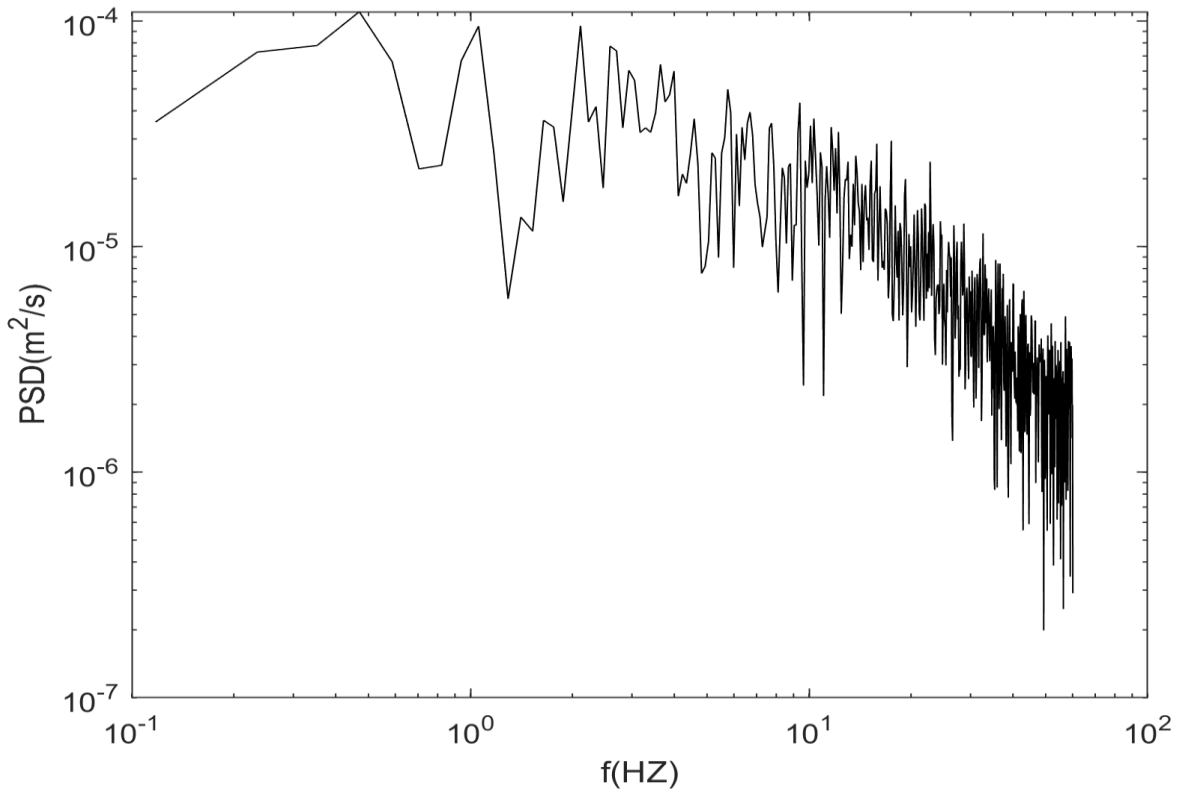


Figure 15: PSD vs f(HZ) at logarithmic scale for point A (5mm from the bottom) for RE=1400

As we can see from the graph above, from ($f = 50.6202$), there is a flat part, which means that region is white noise. So, we draw the graph of PSD vs. frequency for a non-logarithmic scale

(Graph 16) and then calculate the area under the curve, which is the new SD after removing white noise.

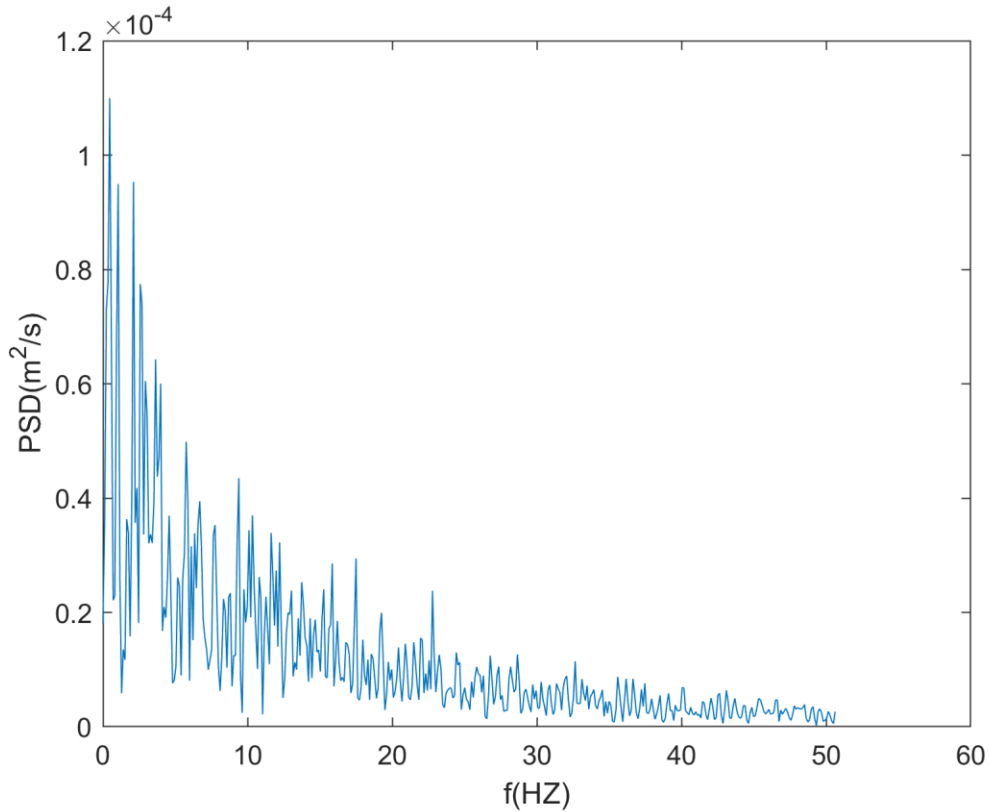


Figure 16: PSD vs f(HZ) at non logarithmic scale for point A (5mm from the bottom) for RE=1400.

After removing white noise, we calculate the turbulent intensities by dividing the standard deviation for all Reynolds numbers before and after removing white noise by the maximum mean velocity. This maximum mean velocity is for Point A at RE=1800, which is equal to 0.48837. The results are shown in Figure 17. (Red curve =before removing white noises, blue curve=after removing white noises)

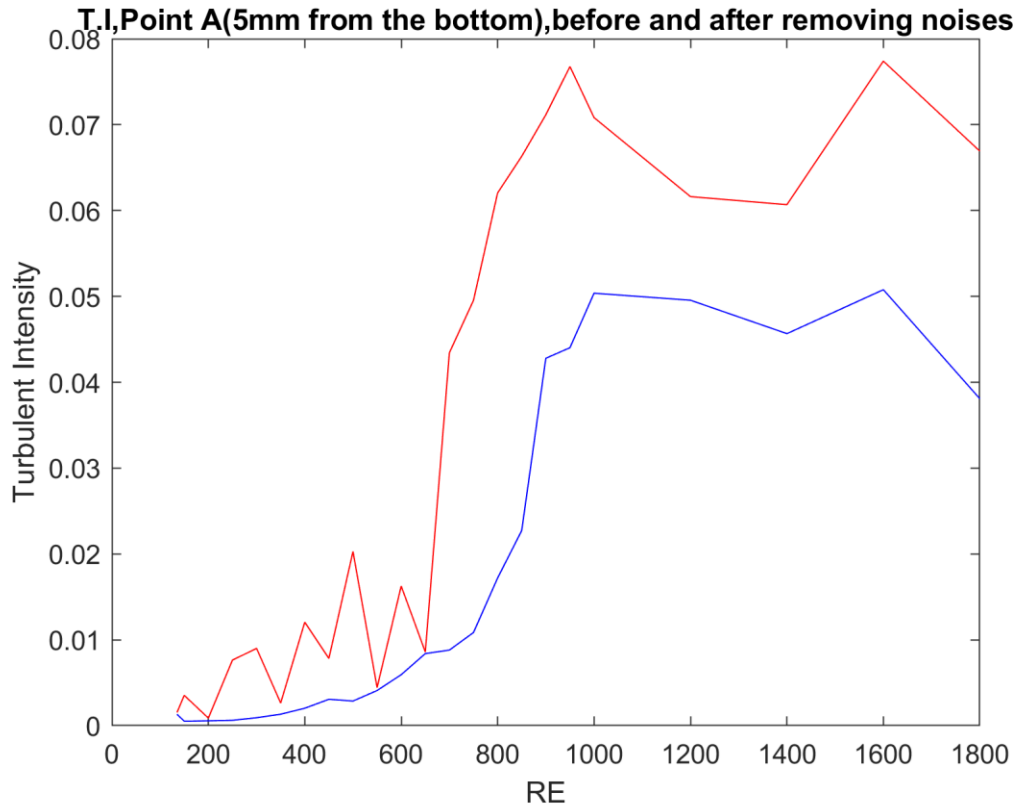


Figure 17: turbulent intensity (T.I) vs RE, for Point A before and after removing white noises.

As evident from the table, there is a clear correlation between Reynolds number and standard deviation. As Reynolds number increases, the standard deviation also tends to increase. And for all Reynold numbers after removing white noises the standard deviation decreases.

4.2: Point B (2.5 mm from the bottom):

The following two figures illustrate the velocity time series for the lowest and highest Reynolds numbers at point B.(figure.15,16)

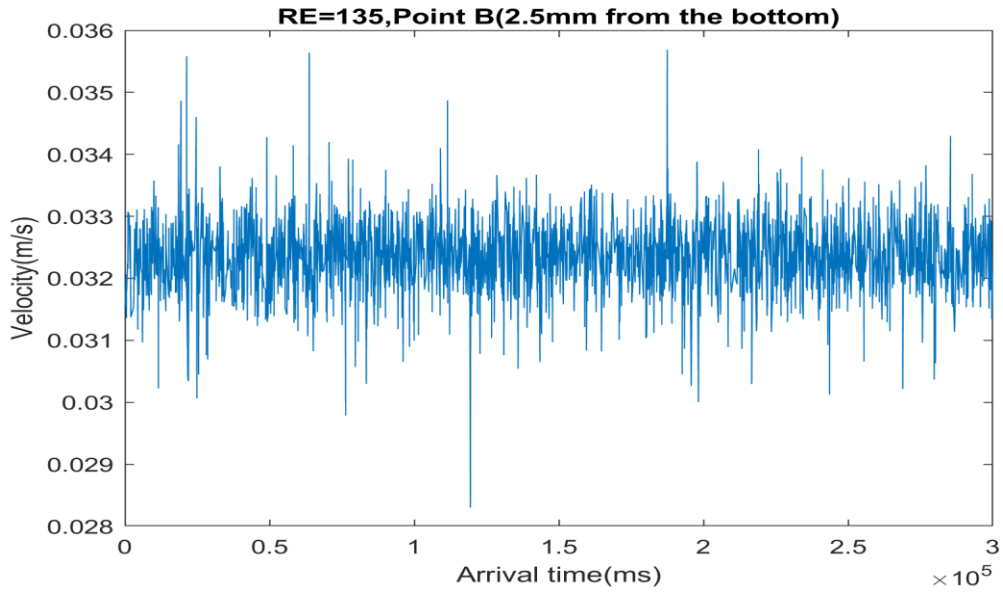


Figure.18: Velocity vs Time for Re=135, Point B(2.5 mm from the bottom)

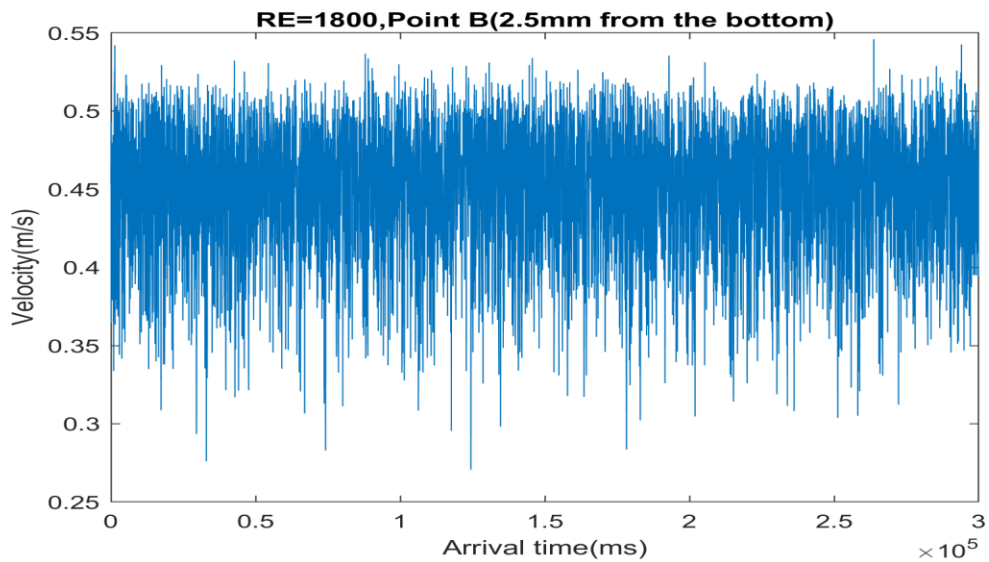


Figure.19: Velocity vs time for Re=1800, Point B (2.5 mm from the bottom)

Exactly like point A, the velocity vs time graph for point B has more fluctuations for higher Re.

Similar to Point A, we have compiled a table of Reynolds numbers, bulk velocities, mean velocities, and standard deviations before and after removing white noises for Point B(2.5 mm from the bottom).(Table.2).

Test	Re	Bulk velocity(m/s)	Mean velocity(m/s)	SD(before removing white noises)	SD(after removing white noises)
1	135	0.027	0.032066	0.0030675	0.000444
2	150	0.03	0.036289	0.0023469	0.000381
3	200	0.04	0.050296	0.0041047	0.000658
4	250	0.05	0.063786	0.0045576	0.000763
5	300	0.06	0.075782	0.0058405	0.0009
6	350	0.070	0.08802	0.0071945	0.0011
7	400	0.080	0.10154	0.0093664	0.0015
8	450	0.09	0.10962	0.013289	0.0030
9	500	0.1	0.12172	0.01256	0.0055
10	550	0.11	0.13597	0.017552	0.0084
11	600	0.12	0.14928	0.023566	0.0104
12	650	0.13	0.16976	0.011992	0.0069
13	700	0.14	0.18751	0.03258	0.0078
14	750	0.15	0.19752	0.040564	0.0090
15	800	0.16	0.21436	0.040572	0.0289
16	850	0.17	0.23211	0.043627	0.0285
17	900	0.18	0.23512	0.045705	0.0298
18	950	0.19	0.24999	0.045681	0.0312
19	1000	0.2	0.26635	0.047578	0.0317
20	1200	0.24	0.30267	0.047615	0.0316
21	1400	0.28	0.3526	0.057507	0.0390
22	1600	0.32	0.39783	0.05828	0.0361
23	1800	0.36	0.44554	0.06363	0.0411

Table.2: Point B, Re, Bulk velocity, Mean velocity, Standard deviation

As evident from the table, there is a clear correlation between Reynolds number and standard deviation like point A. As Reynolds number increases, the standard deviation also tends to increase.

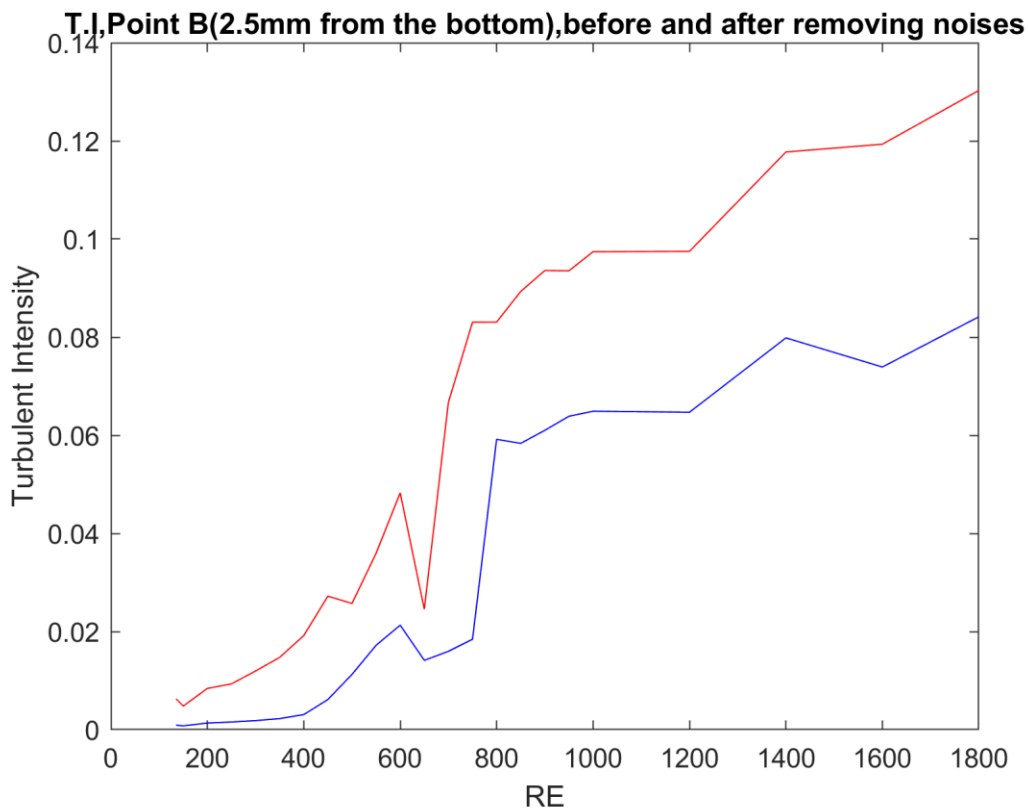


Figure 20: turbulent intensity (T.I) vs RE, for Point B, before and after removing white noises.

Like point A, at point B turbulent intensity has a higher value for before removing white noises than after removing.

4.3: Comparison of Point A and Point B:

At the figure 21 the standard deviation after removing white noises for both points are drawn.

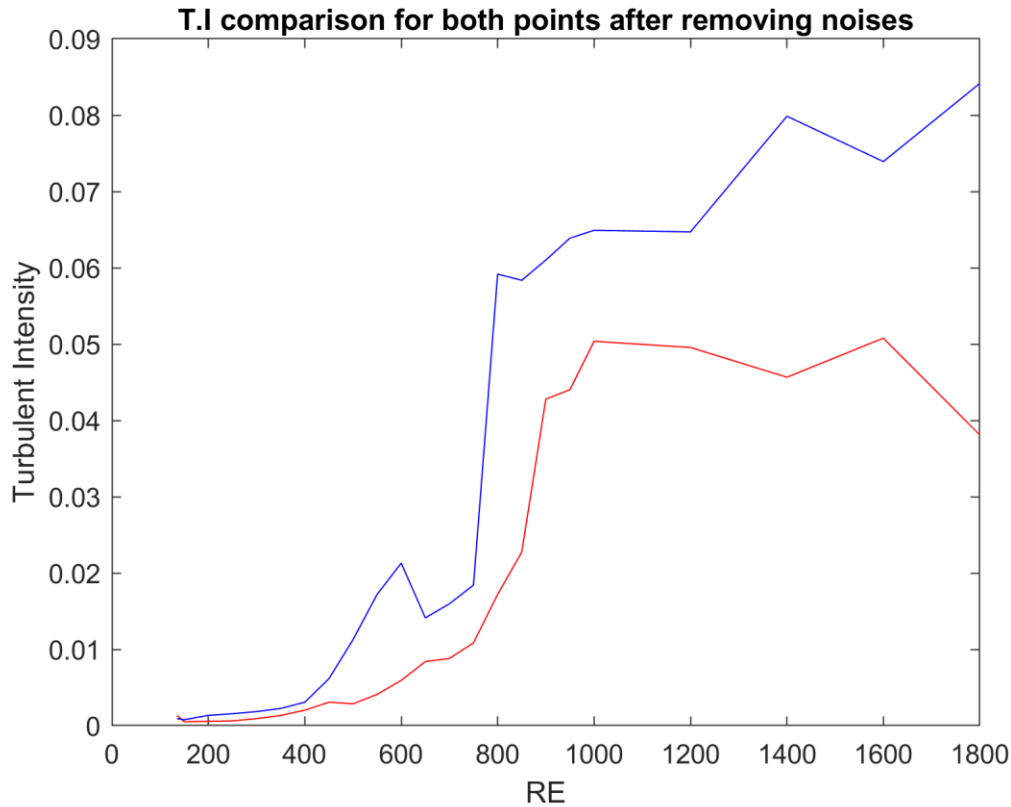


Figure 21: T.I vs Re comparison, for points A(red), B(blue), after removing white noises.

By comparing the graphs of turbulent intensity versus Reynolds number for both points, we can conclude the following:

- **Laminar Regime:** For both Point A and Point B, the flow regime is laminar between Reynolds numbers 135 and 650.
- **Transitional Regime:** A sharp increase in turbulent intensity occurs between Reynolds numbers 650 and 1000, indicating the transition from laminar to turbulent flow.
- **Turbulent Regime:** Reynolds numbers between 1000 and 1800 correspond to the turbulent regime, where turbulent intensity remains relatively constant.

Additionally, although Point A exhibits higher velocities, Point B demonstrates a higher standard deviation. This suggests that Point B has a greater fluid mixing capacity.

Conclusion:

In this study, we investigated turbulent intensity in a section test using fluid water, analyzing velocity time series data to determine the relationship between Reynolds number and flow regime. Our findings highlight the critical role of turbulent intensity in identifying different flow regimes within the fluid.

Our results indicate that the flow regime is laminar for Reynolds numbers between 135 and 650, transitional between 650 and 1000, and turbulent for Reynolds numbers higher than 1000. Interestingly, while the center velocity is higher than at other points, the turbulent intensity at point B (2.5 cm from the bottom) is consistently higher for each Reynolds number.

Understanding and quantifying turbulent intensity is crucial for optimizing water filtration systems. Turbulence affects mixing and transport properties, influencing filtration efficiency. Excessive turbulence can also damage filters. Therefore, maintaining a specific turbulent intensity range is essential for optimal filter performance.

ACKNOWLEDGEMENT:

I would like to express my deepest gratitude to my family for their unwavering support and encouragement throughout this journey. Your love and belief in me have been my greatest source of strength.

To my sibling, thank you for always being there, offering your understanding and patience during the most challenging times. Your support has been invaluable.

I am profoundly grateful to my professor, **Prof. Costantino Manes**, for his guidance, wisdom, and insightful feedback. Your mentorship has been instrumental in the completion of this thesis.

Thank you all for your contributions to this achievement.

REFERENCES :

- 1) Doolan, C., & Moreau, D. (2022). Flow noise: Theory. In Handbook of Open, Distance and Digital Education (pp. 71-105). Springer, Singapore. https://doi.org/10.1007/978-981-19-2484-2_6
- 2) Chung, T. S., & Lu, Z. (2000). The effect of shear rate on gas separation performance of cellulose acetate hollow fiber membranes. *Journal of Membrane Science*, 167(1), 1-13. [https://doi.org/10.1016/S0376-7388\(99\)00284-7](https://doi.org/10.1016/S0376-7388(99)00284-7)
- 3) Monty, J. P. (2005). *Developments in smooth wall turbulent duct flows* (Doctoral dissertation). The University of Melbourne, Department of Mechanical and Manufacturing Engineering.
- 4) Zhang, B., Xu, D., Ji, C., & Ran, Q. (2024). Investigation on the width-to-depth ratio effect on turbulent flows in a sharp meandering channel with periodic boundaries using Large Eddy Simulations. *Research Square*.
- 5) Lu, W., Nguyen, Q. D., Chan, L., Lei, C., & Ooi, A. (2023). Flows past cylinders confined within ducts: Effects of the duct width. *International Journal of Heat and Fluid Flow*, 95, 109208. <https://doi.org/10.1016/j.ijheatfluidflow.2023.109208>